

JI-WON YU<sup>\*,\*\*</sup>, SANG-HOON CHOI<sup>\*,\*\*</sup>, JAE-JIN SIM<sup>\*</sup>, JAE-HONG LIM<sup>\*,\*\*</sup>, KYOUNG-DEOK SEO<sup>\*,\*\*</sup>, SOONG-KEON HYUN<sup>\*\*</sup>, TAE-YOUB KIM<sup>\*\*\*</sup>, BON-WOO GU<sup>\*\*\*</sup>, KYOUNG-TAE PARK<sup>#</sup>

## FABRICATION OF 4N5 GRADE TANTALUM WIRE FROM TANTALUM SCRAP BY EBM AND DRAWING

Electron beam melting (EBM) is a useful technique to obtain high-purity metal ingots. It is also used for melting refractory metals such as tantalum, which require melting techniques employing a high-energy heat source. Drawing is a method which is used to convert the ingot into a wire shape. The required thickness of the wire is achieved by drawing the ingot from a drawing die with a hole of similar size. This process is used to achieve high purity tantalum springs, which are an essential component of lithography lamp in semiconductor manufacturing process. Moreover, high-purity tantalum is used in other applications such as sputtering targets for semiconductors. Studies related to recycling of tantalum from these components have not been carried out until now. The recycling of tantalum is vital for environmental and economic reasons. In order to obtain high-purity tantalum ingot, in this study impurities contained in the scrap were removed by electron beam melting after pre-treatment using aqua regia. The purity of the ingot was then analyzed to be more than 4N5 (99.995%). Subsequently, drawing was performed using the rod melted by electron beam melting. Owing to continuous drawing, the diameter of the tantalum wire decreased to 0.5 mm from 9 mm. The hardness and oxygen concentration of the tantalum ingot were 149 Hv and less than 300 ppm, respectively, whereas the hardness of the tantalum wire was 232.12 Hv. In conclusion, 4N5 grade tantalum wire was successfully fabricated from tantalum scrap by EBM and drawing techniques. Furthermore, procedure to successfully recycle Tantalum from scraps was established.

*Keywords:* Electron Beam Melting, Drawing, Tantalum Scrap, Recycling, High-Purity

### 1. Introduction

Tantalum (Ta) is a refractory metal and shows outstanding chemical and physical properties such as low temperature coefficient of resistance ( $0.00347 \Omega/\Omega K$ ), stable specific resistance ( $131 \mu\Omega/\text{cm}$ ), high density ( $16.65 \text{ g/cm}^3$ ), high melting temperature ( $3017^\circ\text{C}$ ), and high corrosion resistance [1]. Therefore, high-purity tantalum is utilized as a sputtering target, inkjet print head, and in memory chips and microelectronics devices [2,3]. Tantalum oxide of purity 4N5 is generally used in acoustic and electro-optic components [4]. With the growing use of electronic devices, the demand for tantalum capacitors has increased, owing to their high capacity and thermal stability compared to other capacitors. Although an efficient recycling process for tantalum capacitors has not been established thus far, it is necessary, to recycle tantalum from condensers and other scrap [5]. Most tantalum applications require the removal of Al, Fe, Cu, Mn, Cr, Ni, Nb, Na, Li, K, Ti, W, Mo, Si, U, and Th impurities to ppb/ppt levels for high electronic performance [6]. Recycling technologies for tantalum metal include hydrometallurgy, which involves the separation and purification of tantalum metal from tantalum scrap through chlorination [5]; reduction of  $\text{Ta}_2\text{O}_3$  by carbon calcium [7]; reduction of hydrogen by  $\text{TaCl}_5$  [8]; molten

salt electrolysis of  $\text{K}_2\text{TaF}_7$  or reduction by sodium [9,10]; and melting techniques using a high-energy heat source for purification, such as plasma arc melting (PAM), vacuum arc remelting (VAR), and electron beam melting (EBM) [4,11,12]. Pyrometallurgical techniques like alumino-thermic, magnesio-thermic, calcio-thermic, and sodium reduction have not been able to reduce the metallic impurities in tantalum below a few tens of ppm [13-16]. Furthermore, these techniques require a diluent to control the heat of reaction during the experiment [17], and the purity of the recycled powder is approximately 2N (99%) to 3N5 (99.95%), which is not suitable for our study that requires high-level purification. It has to be reached more than 3N5 of purity to apply raw materials of lamp or semiconductor [18,19] which is one of the high-end applications among the Ta related materials as well as various shapes are required such as plate, wire, rod, wire and etc. Objective of our research is to develop recycling technology for tantalum scrap. Purity has to show higher than 3N5 that is the minimum requirement for lamp or target materials for semiconductor process and Drawing was performed to produce wire for applying lithography lamp that is the original source of scrap. Moreover, 4N5 and more grade tantalum is the highest quality among the Ta related component. Therefore, to achieve purities higher than 4N5, EBM was

\* KOREA INSTITUTE OF INDUSTRIAL TECHNOLOGY, INCHEON, REPUBLIC OF KOREA

\*\* IN-HA UNIVERSITY, INCHEON, REPUBLIC OF KOREA

\*\*\* ECO RECYCLING CO., LTD., INCHEON, REPUBLIC OF KOREA

# Corresponding author: ktpark@kitech.re.kr

deemed appropriate as a high-energy heat source for melting and purifying, compared to other hydro- or pyro-metallurgical techniques. High-purity tantalum typically manufactured by high-energy heat source techniques such as EBM, VAR [11], and PAM [12]. EBM in a high-vacuum atmosphere ( $10^{-4}$  torr). They show an excellent refining effect, because most impurities could be removed by the difference of vapor pressure. The impurity removal efficiency of EBM shows higher performance than PAM, because EBM can effectively vaporize metals and organic gas impurities from tantalum metal [4]. Therefore, EBM considered melting techniques of the tantalum scrap. In addition, we confirmed the possibility of recycling tantalum metal from tantalum scrap by manufacturing tantalum wire through EBM and drawing. Up to now, it has steadily been carried out that is studies on the refining of refractory metals using EBM process and the research on the fabrication of wire by plastic working, respectively. However, studies that combine these two processes to recycle refractory metals are insufficient. On the other hand, this research designed to develop technologies for recycling it with upgrade their purity and its wire by combining EBM and drawing technics.

## 2. Experimental

### 2.1. Pre-treatment of raw materials

Tantalum scrap that is spring type from a lithography lamp was as the raw material. The scrap was pretreated with an acidic solution which is aqua regia before EBM. It is a mixture of hydrochloric acid (HCl) and nitric acid ( $\text{HNO}_3$ ), was used as the pretreatment solution, in a molar ratio of 3 : 1. The treatment time was ~50 h, for 1 kg of tantalum scrap. The amount of acid solution was 300 mL per 100 g of tantalum scrap.

### 2.2. Manufacturing of cold hearth and EBM process

A cold hearth was prepared to charge the raw material and was then placed in the EB chamber. It was made copper

materials, and its water pipe was positioned to enclose the charging part. The dimensions of the cold hearth were  $192.5 \text{ mm} \times 20 \text{ mm} \times 20 \text{ mm}$ .

The output power of the EBM equipment was 30 kW, operating voltage was 75 kV, operating current was 22 mA, and process power was 1.5 kW. In the experiment, the degree of vacuum of the EB gun (upper) was about  $10^{-6}$  torr, whereas that in the EB chamber was about  $10^{-4}$  torr. The area of the EB ranged from 5 mm to 10 mm. The focusing current was set to 836 mA. The scan speed was set to 10 mm/s in all experiments. In the EBM process, the scrap was initially charged and melted via EB to form a number of tantalum spots. Afterward more charge was added and melting was again carried out. This process of adding charge and melting was carried out repeatedly for 15 times. During this process, the melt pool was gradually formed. Finally, high purity tantalum ingot was obtained as seen in Fig. 1.

### 2.3. Design of drawing die and drawing process

Drawing was selected as the plastic working technique to fabricate tantalum wires from tantalum ingot. We conducted literature review to establish the drawing process conditions and based on this, drawing die was made. Industrial diamond was selected as the die material. Drawing dies with a diameter range of 0.5 mm to 9 mm were fabricated. Subsequently, tantalum wires of similar diameter were drawn using these dies.

### 2.4. Analysis technique

The impurities on the surface of the scrap were analyzed qualitatively and quantitatively by Inductively Coupled Plasma Mass Spectrometry (ICP-MS). The detection limit in ICP-MS was 0.1 ppb. The purity, hardness, and oxygen concentration of the tantalum ingot were analyzed. The purity of the tantalum ingot was determined by glow discharge mass spectrometry (GD-MS). For the tantalum wire, the diameter, hardness, tensile strength, grain size, crystallographic direction, and strain were analyzed.

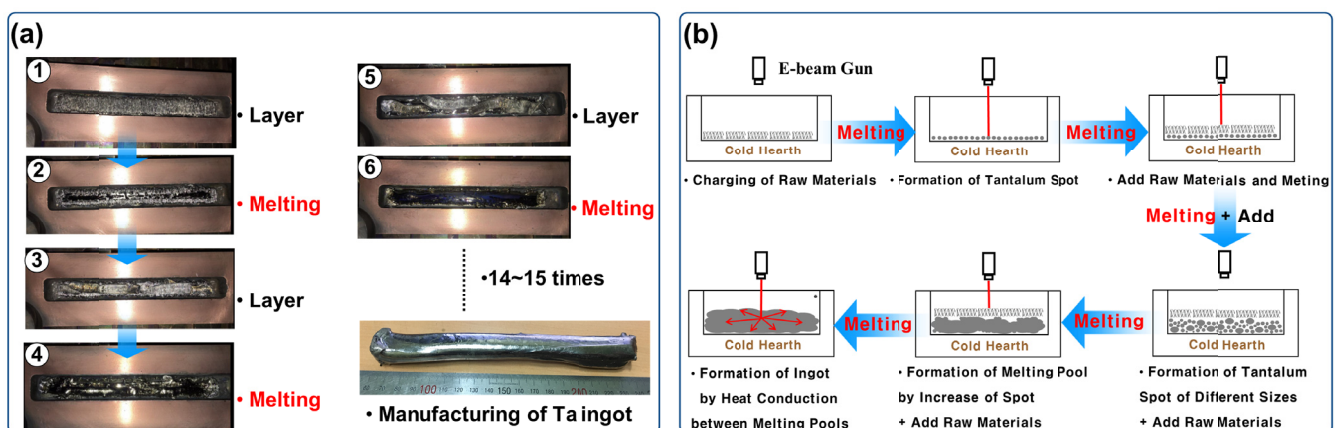


Fig. 1. EBM of tantalum scrap (a) actual melting of tantalum scrap, (b) illustration of melting process of tantalum scrap

### 3. Results and discussion

A lithography lamp is used in the fabrication of semiconductors. During EBM, fume gas is generated from the impurities on the surface of the scrap, which causes reduction of the vacuum degree in the EB chamber and leads to shutdown of equipment. Therefore, the scrap was pretreated with an acidic solution to remove the impurities before EBM. As a result of analyzing the impurities on the surface of the scrap, elements such as W, Ni, Mo, and Fe. Their contents are listed in Table 1. The concentration of impurities was in the order  $W > Fe > Ni > Mo$ ; these impurities could be removed due to the refining effect of EBM.

TABLE 1  
Data for surface impurities on tantalum scrap by ICP-MS

Impurity	Tantalum Scrap (mass-ppm)
W	81.71
Fe	21.55
Ni	1.86
Mo	5.55

The cold hearth material was copper, which has excellent thermal conductivity and can maximize the cooling effect. Moreover, the water pipe in the cold hearth was positioned around the charging area while the cold hearth was being cut by EB, in order to prevent the inflow of water.

EBM (Fig. 1) was used to obtain high-purity tantalum from scrap. It was performed until the raw material fully melted and then tantalum ingot was fabricated. The main process conditions were focusing current, beam current, and scan speed. The focusing current determines the area of the EB; the greater the focusing current, the larger the EB area. The beam current determines the intensity of the EB; the greater the beam current, the higher the intensity of the EB. In addition, it can be adjusted according to the focusing current. For example, when the area of EB is increased by increasing the focusing current, the energy received by the sample is reduced in each area. In order to apply the same intensity of the EB to each area, the beam current must be increased. The scan speed is the rate of scanning the raw materials in the cold hearth, when the EB gun is moved upward, downward, left, and right of the raw materials. As a result, the optimum conditions during EBM is as follows; focusing current, 856-896 mA; beam current, 30-120 mA; scan speed, 10 mm/s.

The purity of the tantalum ingot was analyzed by glow discharge mass spectrometry (GD-MS), which is a non-destructive analytical technique, does not require chemicals for solubility, and can achieve detection limits of less than 0.01 ppm for most impurities [4]. In addition, it is possible to quantitatively detect trace impurities in the refined tantalum matrix. [20-22]. In the tantalum ingots, 0.1 ppm or more of impurities such as W, Ni, Mo, Si, Al, and Fe were detected (Table 2). Excluding these impurities, the purity of the tantalum ingots was respectively 99.99772%, 99.996831%, 99.99884%, 99.99771%, and 99.997388%. Thus, the average purity of the tantalum ingots

was 99.9974% (corresponding to 4N5 or more). The purity data confirmed the excellent refining effect of EBM of the tantalum ingots.

TABLE 2  
GD-MS results for EB-melted tantalum ingots

Impurity	Ta-ingot-01 (mass-ppm)	Ta-ingot-02 (mass-ppm)	Ta-ingot-03 (mass-ppm)	Ta-ingot-04 (mass-ppm)	Ta-ingot-05 (mass-ppm)
W	15.48	19.18	8.9	18.02	18.69
Fe	0.29	0.17	0.97	0.22	0.35
Ni	4.06	5.12	1.58	3.69	4.92
Mo	1.02	1.48	0	0.97	1.6
Si	1.27	3.22	0.15	0	0.38
Al	0.68	2.52	0	0	0.18

The oxygen concentration in the tantalum ingot was also analyzed, for which four samples from the surface of the ingot and one sample from the inner center of the ingot were used. The average oxygen concentration was 257.1 ppm. For the inner sample, the oxygen concentration was 171.5 ppm, whereas for the surface samples, it was 297.8 ppm, 282.6 ppm, 229.3 ppm, and 304.3 ppm. The oxygen concentration of tantalum metal should be less than 200 ppm to fabricate a variety of commercial products [23]. However, all four surface specimens showed oxygen concentrations higher than 200 ppm, exceeding those obtained in other studies. On the other hand, the oxygen concentration of the inner sample was less than 200 ppm; hence, the inner sample can be used in commercial products. These values indicate that the surface was easily oxidized by residual oxygen in the EBM chamber during solidification, whereas the inner part underwent oxidation to a lesser extent. Therefore, to ensure effective plastic working, the surface should be removed in order to eliminate oxygen. The surface of the as-casted ingot of diameter 20 mm was removed to a diameter of 9 mm for use as the raw material in drawing.

In order to reduce the oxygen concentration of the tantalum ingots, it is necessary to remove the oxide through additional EBM. In another study, when EBM was carried out several times, the oxygen concentration of the tantalum ingot decreased more than 500 times compared to that for the case where EBM was performed only once [4].

Hardness was determined by using a Vickers hardness tester by fixing the weight as 0.01 kgf. In addition, the ingot was divided into nine areas and its hardness was measured more than thrice in each area. The average hardness of the tantalum ingot was 148.97 Hv, which is similar to the normal tantalum hardness [24]. Therefore, the tantalum ingot fabricated by EBM can be commercialized for industrial applications.

HSC chemistry was used to calculate the vapor pressures of the impurities in the scrap and the ingot. The calculation was performed according to the temperature of the impurities expected to be present (Fig. 2). The vapor pressures of the impurities are as follows (Fig. 2): manganese,  $7.9 \times 10^{-1}$  torr at

1500°C; aluminum,  $9.7 \times 10^{-3}$  torr at 1500°C; iron,  $2.8 \times 10^{-1}$  torr at 2000°C; and niobium,  $7.6 \times 10^{-3}$  torr at 3000°C. The vapor pressures of tantalum and tungsten are  $4.2 \times 10^{-4}$  torr and  $7.6 \times 10^{-5}$  torr, respectively, at 3000°C. Through the vapor pressure curve, it was confirmed that most of the impurities vaporized before the temperature reaches the melting point of tantalum (3017°C). Furthermore, the niobium and tungsten remaining at around 3017°C are also expected to be vaporized upon increasing the EB intensity in order to raise the melting temperature above 3500°C. However, if we desire the removal of impurities such as niobium and tungsten, it is hard to maintain the tantalum content in the matrix for a constant vapor pressure.

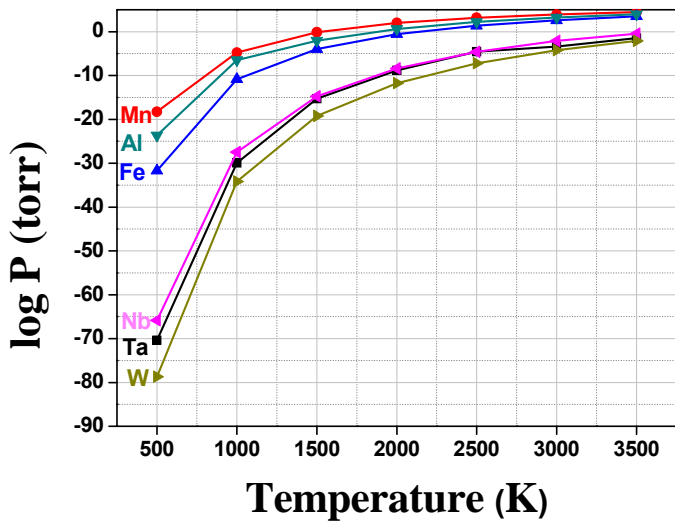


Fig. 2. Vapor pressure-temperature diagram of tantalum and other impurities in tantalum scrap and ingot

If additional EBM at 3500°C or higher temperature is performed, it is expected that most of the impurities can be removed, resulting in an increase in the purity of the tantalum ingot.

Drawing technique involves pulling wire through a drawing die, thereby reducing the diameter of the wire. Drawing is usually performed at room temperature, and is therefore classified as a cold working process. Drawing involves plastic deformation of the metal by exerting compressive forces between the metal and drawing die. The metal is passed through successive drawing dies of decreasing diameter to reduce the diameter of the ingot and wire. The process parameters are die angle, bearing length [25], pulling force, reduction ratio of area, and frictional force (lubrication) [26].

The die angle is the contact angle between the drawing die and drawing material. Drawing dies typically have an angle (semi-angle) in the range of 6-20°. The bearing length is the length of the area of the material passing through the drawing die. The reduction in area is the reduction ratio of the cross-section by drawing, and is calculated as

$$r (\%) = (A_0 - A_1)/A_0 \quad (1)$$

When the die angle is constant, the reduction in the area of the drawing die increases with larger drawing stress. The frictional

force (lubrication) is that between the drawing die and material during drawing. Typically, the surface of a material is lubricated before drawing, to reduce this frictional force, and hence modify the surface roughness and stress on the wire. Tantalum requires surface lubrication during drawing because it is a ductile metal [27].

Cemented carbide and industrial diamond are used as die materials. Cemented carbide is primarily used as a drawing die owing to its excellent strength, toughness, and abrasion resistance. Industrial diamonds have a long life span and are highly resistant to abrasion, cracks, and bearings; they are used to draw fine wires of diameter 1.5 mm to 2 μm.

The optimum die angle used for drawing steel is shown in Fig. 3 [28]. It is determined based on the minimum total energy required for drawing [29]. Furthermore, the optimum die angle can change depending on the change in the area reduction ratio. The values presented in Fig. 3 were calculated for steel, the coefficient of friction ( $\mu$ ) of which is 0.05. In another study, the selection of an angle lower than the optimum die angle reduced the damage to the drawing material without significantly increasing the drawing force. If it is a concern that the stretching of the drawing material is due to the frictional force, then an angle higher than the optimum die angle must be selected [30]. The range of area reduction ratios can be defined based on Eq. (2) (developed by Hill and Tupper), the error of which is less than 1% [31].

$$\alpha (0.230 + \alpha/9) \leq r \leq 2\sin\alpha/(1 + 2\sin\alpha) \quad (2)$$

where  $\alpha$  refers to the semi-angle of the die and  $r$  represents the area reduction ratio. In wire manufacturing, after fixing the area reduction ratio, the die angle is determined by using Eq. (2). When the die angle is fixed, the range of the reduction ratios can be determined.

$$2\sin\alpha/(1 + 2\sin\alpha) \leq r \leq 2.06\alpha - \alpha^2 \quad (3)$$

$$3.5\alpha - 4.9\alpha^2 \leq r \leq 4\alpha - 5\alpha^2 \quad (4)$$

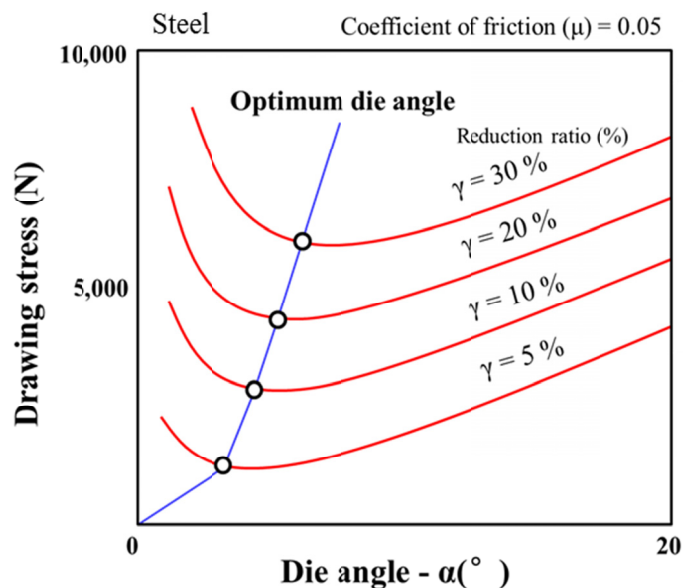


Fig. 3. Relation between die angle and drawing stress during drawing

When designing a die for manufacturing tantalum wires, the die angle can be determined using Eq. (2). Further, the area reduction ratio  $r$  is fixed. When the die angle is fixed, the range of the section reduction ratios  $r$  can be specified. Eq. (2) can be transformed into Eq. (3) and (4), as revealed above. If the area reduction ratio is out of the range, damage of the drawing material is expected [30]. The range of die angles was determined based on the above equations. It was calculated to be  $1.41^\circ$  to  $11.47^\circ$  on the basis of the semi-angle for 5% area reduction ratio. In the initial wire drawing, a drawing die ( $2\alpha$ ) with a diameter of  $12^\circ$  to  $15^\circ$  and a die length of  $0.3d$  were considered. However, the tantalum wire snapped during drawing. To solve this problem, the parameters such as the die material, die angle, and bearing length were reviewed. The tantalum wire can be stretched owing to the friction between the drawing die and the drawing material owing to its ductility. Through electron microscopy, it was confirmed that tantalum was present on the surface of the drawing die. For this reason, the die material was changed to industrial diamond and the die angle was increased ( $12^\circ$  to  $15^\circ \rightarrow 18.23^\circ$ ). On the other hand, the bearing length ( $0.3d \rightarrow 0.2d$ ) was reduced in order to protect the tantalum wire from damage. In the case of ductile metals, there is the possibility of a fault occurring in the wire during drawing due to the drawing force [32]. Therefore, we concluded that shortening the bearing length was advantageous for processing. The area reduction ratio was maintained at 5%, the same as before. The drawing die was designed based on the modified conditions, and the tantalum wire was fabricated as shown in Fig. 4 through drawing. For optimum drawing conditions, a die angle of  $18.23^\circ$  was used whereas bearing length and the area reduction ratio were  $0.2d$  and 5% respectively.

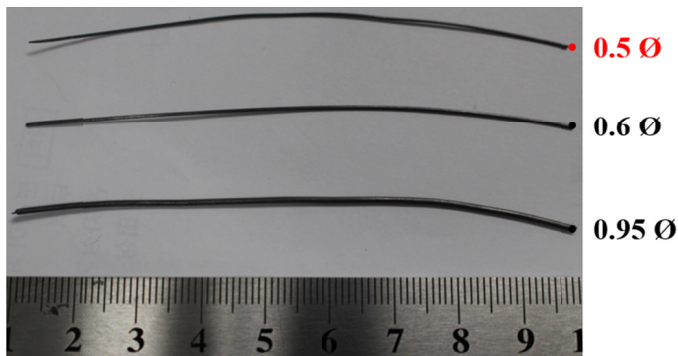


Fig 4. Manufacturing of tantalum wires by drawing

The diameter of the final sample is  $500 \mu\text{m}$ , which is 400 times lower than the diameter of the initial ingot (9 mm). The properties of the tantalum wire such as diameter, hardness, tensile strength, and grain information were analyzed. The diameter of the wire was measured 25 times. The diameter range was  $0.49\text{--}0.51 \text{ mm}$  and the average diameter was  $0.5 \text{ mm}$ .

The hardness was measured after cutting the wire. The measurement was carried out at least 10 times and the weight was fixed at  $0.01 \text{ kgf}$ . Consequently, the hardness was observed to steadily increase from the value for the tantalum ingot to that for the  $0.5 \text{ mm}$  wire sample. The hardness of the ingot is  $148.97$

Hv, while the hardness of the  $0.5 \text{ mm}$  wire is  $232.12 \text{ Hv}$ ; thus, the hardness increased by more than  $80 \text{ Hv}$ .

The tensile strength of the wire was measured 2-4 times and the ultimate tensile strength (UTS), yield strength (YS), and elongation were analyzed as follows (Table 3). The UTS was measured to be  $296.5 \text{ MPa}$  for the  $1.95 \text{ mm}$  wire and  $602.9 \text{ MPa}$  for the  $0.5 \text{ mm}$  wire, and it was confirmed that the value gradually increased by about  $300 \text{ MPa}$ . Similarly, the YS was also measured initially as  $273.8 \text{ MPa}$  for the  $1.95 \text{ mm}$  wire and  $487.9 \text{ MPa}$  for the  $0.5 \text{ mm}$  wire, representing an increase of about  $210 \text{ MPa}$ . The elongation was determined to be  $55.3\%$  for the  $1.95 \text{ mm}$  wire and  $4.71\%$  for the  $0.5 \text{ mm}$  wire. It was confirmed that the value steadily decreased by about  $50\%$ . These results indicate work hardening of the wire during drawing. Furthermore, in order to increase the elongation of the wire, the inner stress must be removed by annealing.

TABLE 3

Variation in mechanical properties during tensile strength test according to the diameter of tantalum

Diameter (mm)	Elongation (%)	UTS (MPa)	Ys (MPa)
1.95	55.3	296.5	273.8
1.90	28.5	313	305.4
1.85	23.3	333.8	307.7
1.75	10.8	373.9	349.7
1.70	8.1	373.5	373.2
1.65	6.4	388.3	375.5
1.55	9.7	386.7	365.1
1.45	7.6	410.6	383.5
1.40	9.8	408.1	382
1.35	7.9	426.2	412.4
1.30	7.5	428.1	412.1
1.25	7	437.7	417.8
1.20	6.7	439.5	429.9
1.10	4.8	449.3	444.7
1.05	5.5	460.1	435.5
1.00	5.6	462.4	436.3
0.95	5.31	475.7	455.2
0.60	4.79	561.6	469
0.50	4.71	602.9	487.9

The properties of the tantalum wire such as grain size and strain were analyzed by EBSD. Fig. 5 shows that the grain size decreased upon drawing. The grain size of each wire was analyzed:  $9.487 \mu\text{m}$  for the  $2.0 \text{ mm}$  wire,  $9.431 \mu\text{m}$  for the  $1.5 \text{ mm}$  wire, and  $2.117 \mu\text{m}$  for the  $0.5 \text{ mm}$  wire. These results indicate that the grains were refined by the plastic deformation that occurred during drawing (Fig. 5(a)). In addition, Fig. 5(b) shows that the strain increased due to the increase in the inner residual stress upon drawing. It can also be seen that the strain in the central area is larger than that at the surface area. According to the results of another study, greater stress was observed at the central area than at the surface area during drawing [33]. In this process, it has also been reported that the crystal orientation of



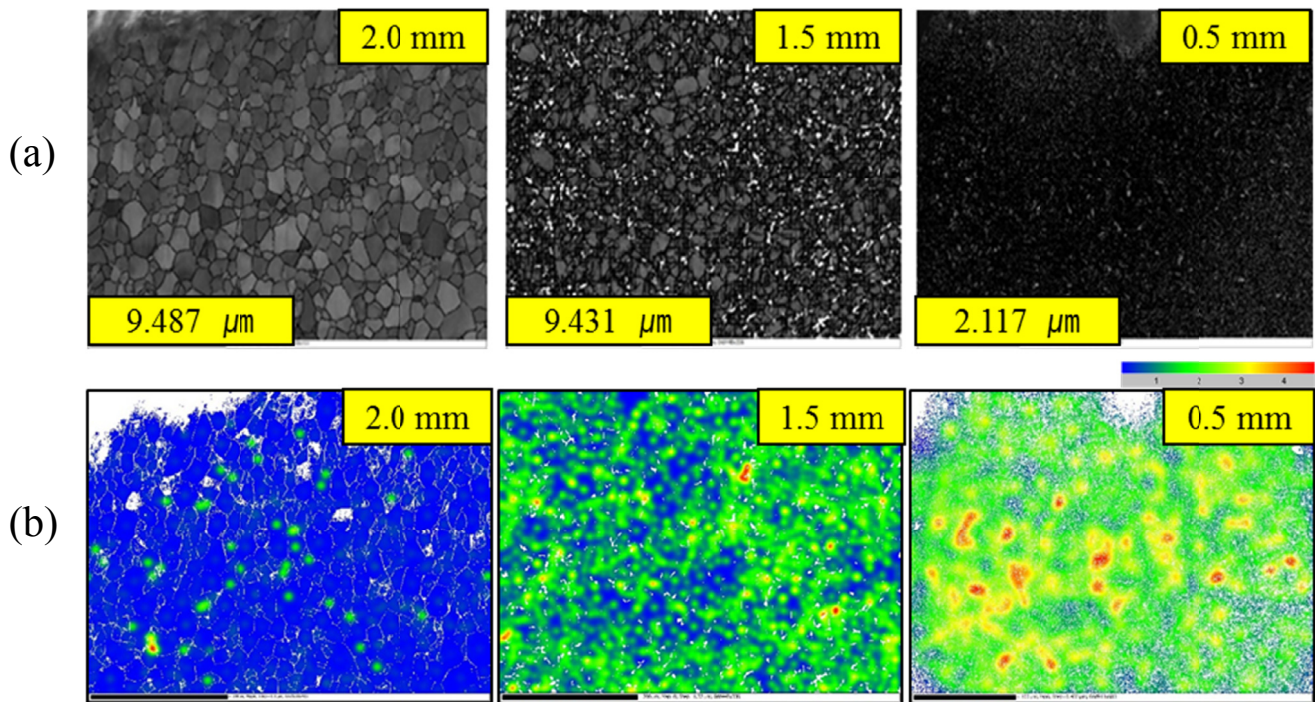


Fig. 5. EBSD analysis of tantalum wire (a) decreased grain size of tantalum wire by drawing, (b) increased strain of tantalum wire by drawing

the central area coincides perfectly with the direction of drawing, while the crystal orientation of the surface area is at a different angle (not parallel) [34]. Based on the analysis data and other studies, it can be inferred that the stress on the central area of the wire is more than that on the surface area and that the strain in the central area is larger than that in the surface area upon drawing. The characteristics of the tantalum ingot and wire were examined by various analysis techniques. Furthermore, the possibility of recycling tantalum scrap was confirmed based on these results.

#### 4. Conclusions

In this study, tantalum wire was successfully fabricated from tantalum scrap by EBM and drawing techniques. The purity of the wire thus obtained was more than 4N5 (99.995%). The impurities present in the tantalum scrap could be removed through pretreatment with an acid solution (aqua regia). GD-MS results showed the excellent refining effect of the EBM. The solidification time of the tantalum ingot can be reduced by fabricating a cold hearth with copper. EBM was carried out in vacuum at 10<sup>-4</sup> torr. The optimum conditions of the EBM were obtained in terms of the focusing and beam currents and scan speed as 856-896 mA, 30-120 mA, and 10 mm/s, respectively. The optimum conditions of the drawing process, such as the die angle, bearing length, and area reduction ratio, were also obtained as 18.23°, 0.2 d, and 5%, respectively. The hardness of the tantalum ingot was determined as 148.97 Hv, while its oxygen concentration was less than 300 ppm. The properties of the ingot such as purity, oxygen concentration, and hardness can be improved by employing an additional EBM step.

The hardness of the 0.5 mm tantalum wire was determined as 232.12 Hv. The UTS, YS, and elongation of the 0.5 mm wire were measured as 602.9 MPa, 487.9 MPa, and 4.71%, respectively, based on tensile strength test. EBSD analysis shows the changes in grain size and strain in the tantalum wire due to drawing. Based on the data obtained for the tantalum ingot and the wire, the possibility of recycling and commercializing the tantalum scrap obtained from the EBM and drawing techniques was confirmed. Up to now, it has steadily been carried out that is studies on the refining of refractory metals using EBM process and the research on the fabrication of wire by plastic working, respectively. However, studies that combine these two processes to recycle refractory metals are absolutely insufficient. On the other hand, this research was designed to develop technologies for recycling and up-cycle of refractory metals by combining EBM and drawing techniques. In addition, it is a consistent process for making ingot from scrap and then manufacturing wire from ingot, which can be used as a useful technology for recycling refractory metals. Not only this, the high-purity tantalum metal recycled in this study can be used as a tantalum spring in lithography lamp as well as other products. If these studies are continuously carried out, commercial recycling process of refractory metals will be established. In addition, it is expected that not only Ta but also all refractory metals such as W, Mo and others will be available.

#### Acknowledgments

This work (Grants No. C0505391) was supported by Business for Cooperative R&D between Industry, Academy, and Research Institute funded by the Ministry of SMEs and Startups(MSS, Korea) in 2017, and partially

supported by the Korea Institute of Energy Technology Evaluation and Planning(KETEP) granted financial resource from the Ministry of Trade, Industry & Energy, Republic of Korea (No. 20165010100870)

## REFERENCES

- [1] M.L.A. Andrade, L.M.S. Cunha, M.C. Silva, Tantalum: The Relevant Brazilian Manufacture, Mining and Metallurgy Bulletin From the Partnership Among BNDES, FINAME and BNDESPAR (2002) (No. 04).
- [2] D.S. Wu, C.C. Chan, R.H. Horng, W.C. Lin, S.L. Chiu, Y.Y. Wu, Appl. Surf. Sci. 144-145 (1999).
- [3] S. Kim, D.J. Duquette, Surf. Coat. Technol. **201**, 2712 (2006).
- [4] G.-S. Choi, J.-W. Lim, N.R. Munirathnam, I.-H Kim, J.-S. Kim, J. Alloys Compd. **469**, 298-303 (2009).
- [5] R. Matsuoka, K. Mineta, T.H. Okabe, EPD Congress 2004 Edited by TMS (The Minerals, Metals & Materials Society), 2004
- [6] R.A. Conte, J.M. Mermet, J.D.A. Rodrigues, J.L.D. Martino, J. Anal. Atom. Spectrom. **12**, 1215 (1997).
- [7] K. Mimura, M. Nanjo, Mater. Trans. **31**, 293-301 (1990).
- [8] CIBA Limited, Belgium patent **625**, 22, 178 (1963).
- [9] T.H. Okabe and D.R. Sadoway: J. Mater. Res. **12**, 3372-3377 (1998).
- [10] D.K. Bose, C.K. Gupta, Min. Pro. Ext. Met. Rev. **22**, 389 (2001).
- [11] A.R. Moss, D.T. Richards, J. Less-Common Met. **2**, 405 (1960).
- [12] D. Elanski, J.-W. Lim, K. Mimura, M. Isshiki, J. Alloys Compd. **413**, 251 (2006).
- [13] M. Baba, R.O. Suzuki, J. Alloys Compd. **392**, 225 (2005).
- [14] C.K. Gupta, P.K. Jena, J. Less-Common Met. **8**, 90 (1965).
- [15] B. Yuan, T.H. Okabe, J. Alloys Compd. **443**, 71 (2007).
- [16] I. Park, T.H. Okabe, Y. Waseda, J. Alloys Compd. **280**, 265 (1998).
- [17] Tantalum-Niobium International Study Center (TIC) Bull. 104 (1998).
- [18] S. Hayashida, I. Kirino, Indus. Rare Metals **115**, 31 (1999).
- [19] <http://www.goodfellow.com/E/Tantalum-Wire.html>
- [20] H.R.Z. Sandim, J.P. Martins, A.L. Pinto, A.F. Padilha, Mater. Sci. Eng. A **392**, 209 (2005).
- [21] J.S. Becker, H.J. Dietze, Spectrochim. Acta B 1475-1506 (1998).
- [22] T. Saka, M. Inoue, Anal. Sci. **16**, 53 (2000).
- [23] W. Vieth, J.C. Huneke, Spectrochim. Acta B **46**, 137 (1991).
- [24] Material Property Data (<http://www.matweb.com/>)
- [25] C.-S. Moon, N.-S. Kim, J. Mech. Sci. Technol. **26** (9), 2903-2911 (2012).
- [26] A.L.R. De Castro, H.B. Campos, P.R. Cetlin, J. Mater. Proc. Technol. **60**, 179-182 (1996).
- [27] K.D. Moser, J. Minerals, Metals & Mater. Soc. **51** (4), 29-31 (1999).
- [28] 6th Division-Drawing Process, Plastic Processing Technology Series, J. Japan Soc. Technol. Plast. (1990).
- [29] G. Deep, J. C. Farge, P. Chollet, E. Gervais, J. Appl. Metal Working **2** (4), (1983).
- [30] T. Massé, L. Fourment, P. Montmitonnet, C. Bobadilla, S. Foissey, Int. J. Mater. Form, **5** January 2012 (in press).
- [31] A.P. Green, R. Hill, J. Mech. Phys. Solids **1**, 31-36 (1952).
- [32] A.K.F. Hassan, A.S. Hashim, Univ. J. Mech. Eng. **3** (3), 71-82 (2015).
- [33] S.-K. Lee, D.-W. Kim, M.-S. Jeong, B.-M. Kim, J. Mater. Design **34**, 363-371 (2012).
- [34] T.-Z. Zhao, G.-L. Zhang, H.-W. Song, M. Cheng, S.-H. Zhang, J. Mater. Engg. Perf. **23** (9), 3279-3284 (2014).